www.czasopisma.pan.pl PAN www.journals.pan.pl
Opto-Electronics Review 26 (2018) 285–295

Contents lists available at ScienceDirect

Opto-Electronics Review

journal homepage: http://www.journals.elsevier.com/opto-electronics review

Integrated 25 GHz and 50 GHz spectral line width dense wavelength division demultiplexer on single photonic crystal chip

V.R. Balaji [a,*], M. Murugan [b], S. Robinson [c], R. Nakkeeran [d]

[a] Department of Electronics and Communication Engineering, St. Joseph's Institute of Technology, Chennai, 600119, Tamilnadu, India
[b] Department of Electronics and Communication Engineering, Valliammai Engineering College, Kattankulathur, 603203, Tamilnadu, India
[c] Department of Electronics and Communication Engineering, Mount Zion College of Engineering and Technology, Pudukkottai, 622 507, Tamilnadu, India
[d] Department of Electronics Engineering, Pondicherry University, Puducherry, 605 014, India

ARTICLE INFO

Article history:
Received 20 August 2017
Received in revised form 7 October 2018
Accepted 9 October 2018
Available online 6 November 2018

Keywords:
Demultiplexer
Crosstalk
Quality factor
Line width
Cavity

ABSTRACT

We propose a new integrated demultiplexer model using the two-dimensional photonic crystal (2D PC) through the hexagonal resonant cavity (HRC) for the International Telecommunication Union (ITU) standard. The integrated model of demultiplexer for both 25 GHz and 50 GHz has been designed for the first time. The demultiplexer consists of bus input waveguide, drop waveguide, Hexagonal Resonant Cavity (HRC), 6 Air Hole Filter (6-AHF), 7 Air Hole Filter (7-AHF). The 7-AHF is used to filter 25GHz wavelength, and the 6-AHF filter is used to filter 50 GHz wavelength. The Q-factor on the designed demultiplexer is flexible based on the idea of increasing the number of air holes between drop waveguide and resonant cavity. The demultiplexer is designed to drop maximum 8 resonant wavelengths. One side of demultiplexer is able to drop 50 GHz ITU standard wavelengths, which are of 1556.3 nm, 1556.7 nm, 1557.1 nm and 1557.5 nm, and further the other facet is able to drop 25 GHz wavelengths, which are of 1551.4 nm, 1551.6 nm, 1551.8 nm, and 1552.0 nm. The proposed demultiplexer may be carried out within the integrated dual system. This system is able to lessen the architecture cost and the size is miniaturized substantially.

1. Introduction

Optical fiber communications transfer digital data with fewer noises in contrast with the Radio Frequency (RF) technology. However, an individual fiber to each user becomes more difficult and expensive. The solution is routing Single Mode Fiber (SMF) to N number of users. The SMF uses the Wavelength Division Multiplexing (WDM) technology that transfers a number of light waves onto a single optical fiber through different wavelengths [1]. In the receiver end, a transferred light wavelength is routed to individual users with optical demultiplexer. In today's internet world, with increasing number of users, it is imperative for an integrated device to be of low noise, ultra-compact in nanometer range and meet the ITU standards. Therefore, it can be replaced with Photonic Crystals (PCs). PCs are artificial nano structure electromagnetic media with interesting properties like low sharp bend loss and ultra compact size. The concept of Photonic Band Gap (PBG) in PCs plays a dominant role in the application of Photonic Integrated Circuits (PIC). Owing to the interesting properties of collimated light and negative refraction, many optical devices are proposed, such as PC sensors [2], PC splitters [3], PC demultiplexers [4], PC couplers [5], PC wavelength convertors [6], PC channel filters [7], and PC buffers [8]. The PC demultiplexer is an essential component in WDM. The WDM is classified into Dense Wavelength Division Multiplexing (DWDM) and Coarse Wavelength Division Multiplexing (CWDM) based on its channel spacing.

The CWDM of ITU-T G.694.2 standard channel spacing is wide about 20 nm, whose utilization rate of bandwidth is low and DWDM of ITU-T G.694.1 with a standard channel spacing of 0.1 nm, 0.2 nm, 0.4 nm, 0.8 nm, and 1.6 nm has a very high utilization rate of bandwidth. The narrow bandwidth feature of DWDM standard attracts many researchers to improve the DWDM systems. Further improvisation of DWDM technology in fiber optic integrated systems would support different network users on a large scale and concede to transmit the fiber concurrently to customers.

In the literature survey, several attempts have been made to design the PC based optical demultiplexer. The 2DPC based optical demultiplexer has been reported with point/line defects [10–13,17] and resonant cavity [14–16,18] using triangular and square lattice. The PBG is wider in the triangular lattice [9] and the fabrication

* Corresponding author.
E-mail address: balajivr@stjosephstechnology.ac.in (V.R. Balaji).

https://doi.org/10.1016/j.opelre.2018.10.001
1230-3402/

of air holes in the SOI slab is simpler compared to the square lattice. In this work, a triangular lattice is preferred due to aforementioned advantages. A two-channel PC optical demultiplexer has been reported by varying the central point defect, with 20 nm channel spacing and −14 dB crosstalk [10]. The two-channel PC optical demultiplexer designed in a Y shape has a channel spacing of 24 nm and the transmission efficiency of 69% [11]. The two channel PC demultiplexer design consists of two ring resonator with a unique center rod. The design had transmission efficiency, spectral linewidth and crosstalk of 99%, 0.2 nm, −22 dB [12].The two channel demultiplexer design with waveguide and resonant cavity. The wavelength is dropped with changing the central defect at a distance. The design had channel spacing, Q-factor and crosstalk of 0.2 nm,7900 and −22.11 dB [13].The two channel demultiplexer is designed with L3 cavity. The design had transmission efficiency, channel spacing, Q-factor, and crosstalk of 70%, 5.3 nm,1000 and −13.8 dB [14]. The two channel demultiplexer designed with an X shaped cavity. The designed had transmission efficiency, spectral linewidth and Q-factor of 76%, 4.5 nm, and 433 [15]. The four channel demultiplxer is designed with four ring resonator along the unique inner rod radii. The design had transmission efficiency, channel spacing, Q-factor, and crosstalk of 95%, 3 nm, 2600 and −19 dB [16]. The four channel demultiplexer design using waveguide coupler with the separation of dielectric rod in the interaction region. The design had 20 nm channel spacing and 100% transmission efficiency [17]. The four channel demultiplexer is designed with planar PC. The desired wavelength is dropped with changing the radius of the border hole. The design reported 10 nm spectral linewidth and 100% transmission efficiency [18]. The four channel demultiplexer design with three ring resonator with T-shaped. The design reported with higher transmission efficiency of 90% [19]. The four channel demultiplexer is designed using four ring resonator. The design had 90% transmission efficiency, −25 dB crosstalk and Q-factor of 96. [20]. Following the four channel, the demultiplexer is designed with resonant cavity, defect created by radii of two adjacent rods. The design had spectral linewidth, Q-factor, and transmission efficiency of 2.5 nm,796 and 100% [21]

Following that, the four-channel PC optical demultiplexer was proposed with T-branch waveguide with micro resonant cavities, which gives a Q-factor of about 3488, transmission efficiency below 70%, and a channel spacing of around 1 nm [22]. Four channel PC optical demultiplexer is designed with coupling cavities, provides high transmission efficiency of 99% and channel spacing of 20-nm [23]. Another four-channel demultiplexer was proposed with an X-shape ring cavity which gives low transmission efficiency of around 60% and channel spacing of 2.3 nm [24]. The six channel demultiplexer is designed with defect row of photonic crystal. The design had spectral linewidth of 1.4 nm and maximum transmission efficiency of 70% [25]. The six channel demultiplexer is designed with six different cavity. The design had maximum transmission efficiency, crosstalk, and Q-factor of 100%, −29 dB and 2319 [26]. Following that, the six channel demultiplexer design with microcavity. The design had spectral linewidth and transmission efficiency of 2 nm and 90% [27]. The seven channel demultiplexer is designed with Fabry-Perot reflector for the desired wavelength. The design had transmission efficiency of 36%, respectively [28].

The eight channel demultiplexer is designed with quasi square ring resonator along with different inner rod radii. The design had transmission efficiency, spectral linewidth, Q-factor and crosstalk about 96%, 1.4 nm, 1922 and −26.9 dB [29]. The eight channel demultiplexer is designed using square ring resonator. The design had transmission efficiency, spectral linewidth, and Q-factor of 81%,1.8 nm and 825 [30]. The eight channel demultiplexer is designed with dual ring resonator. The design has transmission efficiency, spectral linewidth and Q-factor of 98%,0.4 nm and 3225 [31]. The eight-channel PC optical demultiplexer was reported with multilayer ring resonator that had even channel spacing of 1 nm, unequal spectral linewidth, Q-factor 4320, and transmission efficiency 93% [32].

An eight-channel optical demultiplexer is designed with arc cavity which gives a Q-factor of 4860 and transmission efficiency of 90% [33]. The eight-channel demultiplexer that was designed with point defects gives transmission efficiency of about 94%, and crosstalk around −11.2 dB with a Q-factor of 2200 [34]. Following that, the ten channel demultiplexer is designed with circle oval rods by altering the angle. The design is reported with higher transmission efficiency up to 90% [35]. Following that, a 12-channel DWDM demultiplexer was designed using central defect (Rm) with a high Q-factor of 7890, transmission efficiency, uniform spectral linewidth, and uniform channel spacing of about 0.2 nm, −42 dB [36]. From the literature survey, it has been studied that optical demultiplexers are designed using different shapes and resonant cavities with different lattices, and are reported to have high transmission efficiency, Q-factor and minimal crosstalk. Unfortunately, all reported papers are designed to drop the wavelength in single frequency or random frequency. There is only one attempt with integrated model [37] which shows more crosstalk, low transmission efficiency. However, all reported papers have not given emphasis on many aspects like uniform channel spacing, uniform spectral linewidth, integrated model for multifunction future DWDM systems. To the best of our knowledge, there is no DWDM demultiplexer that has been proposed to realize both 25 GHz and 50 GHz spectral line width demultiplexing in a single slab. However, the increasing trend in PIC has resulted in the lookout for nano compact components with multiple functions.

In this paper, following the work of using parellogram resonant cavity in the signal frequency eight-channel demultiplexer [38], we propose a new integrated model for both 25 GHz and 50 GHz spectrum demultiplexer in a single slab for the four-channel and eight-channel DWDM demultiplexer. The proposed model is designed to work for ITU-T G.694.1 DWDM systems with uniform spectral line width of 0.2 nm and 0.4 nm, average uniform channel spacing, integrated model, high transmission efficiency, high Q-factor of 7800 and low crosstalk between neighboring channels. The proposed models try to enhance the maximum utilization of the SMF by dropping two narrow band spectrums like 0.2 nm and 0.4 nm.

This paper is organized as follows. Section 2 discusses the PBG calculated for the proposed demultiplexer structure using Plane Wave Expansion (PWE) method. The design and the details of four-channel integrated demultiplexer are presented in Section 3. The eight-channel integrated demultiplexer is presented in Section 4. The simulated results for the proposed four-channel and eight-channel integrated demultiplexer are discussed in Section 5. Finally, Section 6 concludes the paper.

2. Photonic crystal geometry

Silicon on Insulator (SOI) substrate is utilized to design the integrated DWDM demultiplexer with triangular lattice. It consists of a thin silicon layer separated from silicon substrate by an oxide layer. This SOI material is well suited for guided optics. The PC design consists of a triangular lattice of 'Si' air holes with a thickness of 220 nm, which is developed above 1000 nm of SiO_2 and 450 nm of Si substrate realized by SOI as shown in Fig. 1(a). The structure that has been used for the design consists of 38 × 38 air holes. The 2DFDTD method is employed to measure functional parameters of the proposed demutiplexer. The refractive index of air/silicon on top layer is of 1/3.48 at 1550 nm and the refractive index of SiO_2 is 1.45.The effective refractive index for the design is of 2.83. The radius of basic

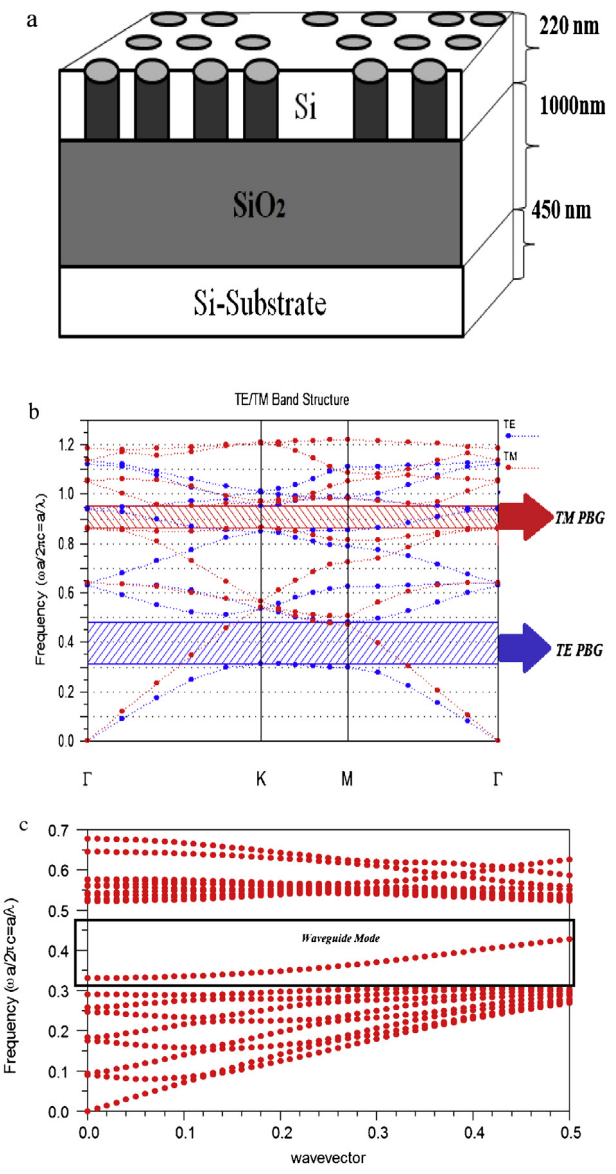

Fig. 1. (a) Pictorial drawing of photonic crystal in Silicon-on-Insultor. (b) Band gap diagram of the proposed 38 × 38 air holes, prior to defects. (c). Band gap diagram of the proposed 38 × 38 air holes after defects.

air holes without defect is of 92 nm and the lattice constant (a) is of 680 nm.

The initial step in designing photonic crystal devices is to determine the PBG of the proposed lattice. The calculation of PBG is done by Plane Wave Expansion (PWE) method [39]. The PWE method is used to calculate the propagation of electromagnetic modes in the periodic and non-periodic structure with the Maxwell's equation. It determines the allowable frequency for light propagation in PC through intact direction. But PWE method is not able to determine the transmission spectrum and reflection spectrum. The FDTD algorthim simulates the propgation of electromagnetic waves inside the SOI lattice. Transmission and back reflection spectrum are determined with FDTD.

Figure 1(b) shows the PBG for 38 × 38 air holes before introducing the defects which has two PBG regions(1 TE & 1 TM) in the band diagram. The TE PBG normalized frequency lies between $0.35 < a/\lambda < 0.49$ and 1387 nm $< \lambda <$ 1942 nm. The TM PBG normalized frequency lies between $0.88 < a/\lambda < 0.98$ and 693 nm $< \lambda <$ 772 nm. The light signal is not propagated inside the structure over the wavelength range. However, the signal will be propagated inside the structure in the aforementioned wavelength range by introducing the line and point defects.

The familiar Maxwell equations are given by the equations:

$$\frac{\partial E}{\partial t} = \frac{1}{\varepsilon}\nabla \times H - \frac{\sigma}{\varepsilon}E \tag{1}$$

$$\frac{\partial H}{\partial t} = -\frac{1}{\mu}\nabla \times E. \tag{2}$$

Where, E is the electric field, H is the magnetic field, σ is the conductivity of the medium, μ is the permeability of the medium, and ε is the permittivity of the medium. Maxwell curl equations with the flux density written as [40,41]

$$\frac{\partial D}{\partial t} = \nabla \times H \tag{3}$$

$$\frac{\partial H}{\partial t} = -\frac{1}{\mu}\nabla \times E \tag{4}$$

$$D(\omega) = \varepsilon_0 \varepsilon_r^*(\omega) E(\omega). \tag{5}$$

Where, ε_0 is the permittivity of a vacuum and ε_r is the permittivity of the medium, respectively. Equations (3) and (4) are regardless to the medium. In the proposed design normalized unit is used with PML. Normalized field are obtained with:

$$\tilde{E} = \sqrt{\frac{\varepsilon_0}{\mu_0}}E \tag{6}$$

$$\tilde{D} = \sqrt{\frac{1}{\varepsilon_0 \mu_0}}D. \tag{7}$$

Maxwell curl equations express in a normalized flux density, therefore equation becomes independent of material properties and Disperson, non-linearity of the material with the equation:

$$D(\omega) = \varepsilon_0 \varepsilon^r(\omega) E(\omega), \tag{8}$$

where D is the flux density.

Equation (8) is in a frequency domain, Maxwell's curl equations with normalized flux density in FDTD'.

The efficient way in manipulating the light is with introducing defects in the symmetry triangular lattice. The introducing defects in the lattice break the symmetry structure of the lattice [42]. The non symmetry structure are used to design bus waveguide, resonator, AHF and output waveguide in the proposed design.

Band diagram of the proposed designed demultiplexer after introducing the defects is as shown in Fig. 1(c). The guided mode in PC demultiplexer is obtained using PWE. PC ability to trap the wavelength by point defect cavity (6-AHF & 7 AHF) in the proposed design. The point defect is introduced in design, a single waveguide mode propagates inside the proposed PBG.

3. Proposed four- channel integrated demultiplexer

Figure 2 shows the architecture for DWDM network which consists of Integrated DWDM Multiplexer / Demultiplexer, SMF and Amplifier. The user sends data with 8 resonant wavelengths with integrated spectral line width (25 GHz/50 GHz) from the main office. From the main office data is transmitted with SMF for long distance communication with amplifier. The amplifier is used to avoid the signal degradation below the threshold level. The multiplexed output from SMF split with PC demultiplexer to different 8 end user with the needed resonant wavelength. Proposed demultiplexer can split the broad and narrow wavelength at the same time. This system drastically reduces structural design costs. The core task in the demultiplexer is separating unique adjacent wavelengths with the center resonant wavelengths with less crosstalk.

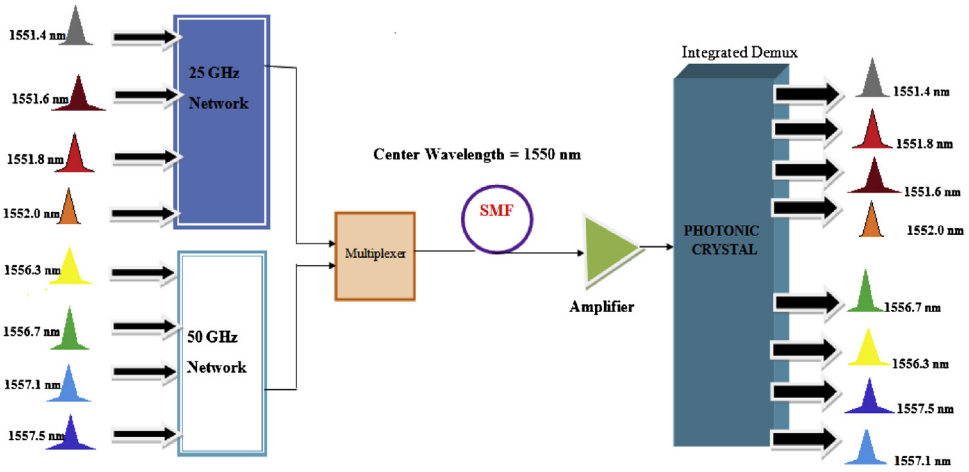

Fig. 2. Proposed architecture for the integrated demultiplexer.

The wavelength spacing will be small in 25 GHz system in comparison with 50 GHz system, and it is required to increase Q-values from the filter. The filter Q-factor can be raised by increasing the number of air holes between drop waveguide and resonant cavity. Later, horizontal/vertical loss needs to be reduced and finally, air hole parameters are optimized with resonant wavelength.

The proposed four-channel integrated demultiplexer consists of two Hexagonal Resonant Cavity (HRC) where on one side HRC is designed to drop two distinct wavelengths with a bandwidth of 25 GHz and on the other side it satisfies the standard of 50 GHz. Figure 3 shows the sectional view of two HRCs using two-hexagonal resonators. One side of demultiplexer consists of one HRC which encompasses the hexagonal ring resonators with two 6-AHF and two dropping waveguides. The hexagonal resonator is an optical waveguide in which electromagnetic waves resonate with constructive interference by a phase shift equal to the multiple of 2π. 6-AHF with point defects is introduced. The radius of air hole is increased to increase the dielectric constant of the filter air holes. Resonant wavelength swings to a higher value proportional to the dielectric strength. The unique radius of AHF filter is optimized after 500 iterations to drop the desired DWDM wavelength. The bottom HRC consists of hexagonal ring resonator with two 7-AHFs and two dropping waveguides. 7-AHF is used to filter the 25 GHz spectral linewidth wavelength with a unique air hole radius.

The radius of 6-AHF determines with R1 and 7-AHF determines with R2. The size of 6- AHF and 7-AHF is altered with changing the radius of air holes. Through altering the size of the radii, dielectric constant of the cavity is varied and it leads to different wavelength couple to output waveguide through 6-AHF and 7-AHF.

The diameter (D1) and the radius (R1)

$$\text{of 6-AHF } D1 = 2a \text{ and } R1 = a. \tag{9}$$

The diameter (D2) and the radius (R2)

$$\text{of 7-AHF } D2 = 2a \text{ and } R2 = a-r. \tag{10}$$

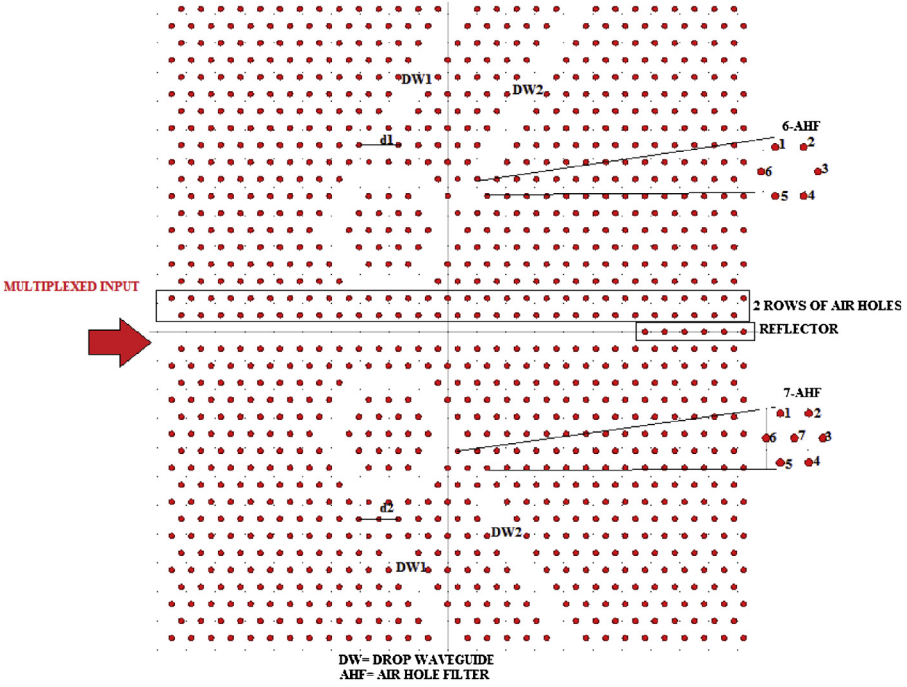

Fig. 3. Proposed four-channel integrated demultiplexer.

Table 1
Resonant wavelength, cavity size, radius of defect air hole, spectral linewidth, Q-factor and efficiency of the proposed four-channel demultiplexer.

Channel Spacing	Defect Radius (nm)	Cavity Size	DWDM CHANNELS		Spectral Linewidth ($\Delta\lambda$) in (nm)	Q-Factor	Transmission Efficiency (%)
			7-AHF (25 GHz)	6 AHF (50 GHz)			
0.2 nm	81.8 (C1)	588 nm	λ_1 1552.2 nm	NA	0.2 nm	7756	95
	83 (C2)	588 nm	λ_2 1552.4 nm	NA	0.2 nm	7757	95
0.4 nm	89.2 (C1)	680 nm	NA	λ_1 1554 nm	0.410 nm	3889	98
	90.4 (C2)	680 nm	NA	λ_2 1554.4 nm	0.412 nm	3890	98

a is the lattice constant of air holes, r is the radius of point defect air holes.

For realizing the wavelength selection filter, hexagonal resonator, 6-AHF, and 7-AHF have been introduced. Hexagonal resonator provides a better confinement of light in vertical direction. 6-AHF provides broad 50 GHz spectral linewidth. 7-AHF provides narrow 25 GHz spectral linewidth with an increase in the count of holes around the drop waveguide. The desired wavelength is dropped with the adjusting values of 6 air hole filter (6-AHF) are C1 = 81.8 nm, C2 = 83 nm. The behavior is realized with changing the radius of AHF, optimum radius is determined by varying the size from 40 nm to 96 nm, by measuring the intensity of the light. For the point defect of radius of 81.8 nm, high Q-factor resonant wavelength is obtained at 1552.2 nm. Similarly, other detailed performance parameters are provided in Table 1.The radii of 7 air hole filter for dropping 0.2 nm wavelengths are C1 = 89.2 nm, C2 = 90.4 nm. The footprint of the proposed device is of 330.48 μm^2.

The radius of the rods is optimized under 500 iterations with the change of different criteria like lattice constant, rod characteristics and refractive index property to obtain high Q-factor and group velocity, narrow spectral line width and uniform channel spacing.

The multiplexed signal is traveled through SMF to the Photonic Crystal Waveguide (PCWG) which is coupled with the taper [43] to match a different width of the SMF. As per our objective, the channel separation is sufficient for real time applications with the insertion loss of 0.5 dB.

4. Proposed-integrated eight-channel demultiplexer

Figure 4 shows the schematic view of eight-channel integrated demultiplexer. The integrated demultiplexer utilizes 38×38 air holes; with a footprint size of 481 μm^2. The design consists of one bus waveguide, eight drop waveguides, four HRCs, four 6-AHF and 7-AHF, and reflector air holes.

Two hexagonal resonant cavities (HRC 1 and HRC 2) positioned on one side of the bus waveguide are optimized to drop 50 GHz channels ($\lambda_1, \lambda 2, \lambda 3, \lambda 4$) and the remaining resonant cavities (HRC 3 & HRC 4) positioned on the bottom of bus waveguide are optimized to drop 25 GHz channels (λ_1, $\lambda 2$, $\lambda 3$, $\lambda 4$). A high spectral narrow linewidth is obtained by increasing the number of air holes between the drop waveguide and the resonator. The proposed design is extremely useful in dual network implementation.

In the 25 GHz demultiplexer each HRC has two 7-AHF placed at the end of HRC and nearer to the dropping waveguide. The inter channel crosstalk between the channels is reduced with placing five rows of air holes between the adjacent channels. Similar principle is followed for the 50 GHz demultiplexer. Each HRC has two air hole filters. The radii of 6 air holes is varied to filter the unique 50 GHz wavelength from the hexagonal resonator and dropped to the output waveguide with limited side bands. Similar principles are followed for 7-AHF apart from increasing the number of holes to get high Q-factor. The radii of 6-AHFs for the channels are C1 = 77 nm, C2 = 78.2 nm, C3 = 79.4 nm, and C4 = 80.6 nm. The radii of 7-AHFs for the channels are C1 = 95.6 nm, C2 = 96.8 nm, C3 = 98 nm and C4 = 99.2 nm.

The separation of resonant wavelengths from the integrated demultiplexer was tried in different scenarios to obtain the best way as in the proposed model. In the proposed model two possibilities to filter the desired wavelength were tried; the first one being, increasing the inner air holes in the HRC along with AHF radius and the second, changing the AHF filter radius. Increasing the inner air holes along with AHF in each channel is not a good choice because

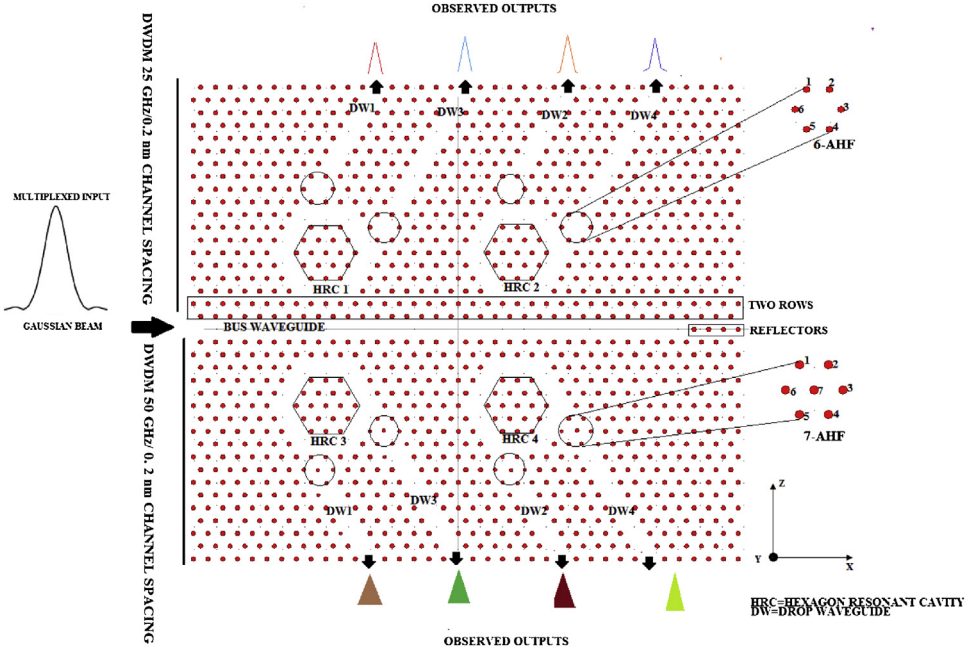

Fig. 4. Proposed eight-channel integrated demultiplexer.

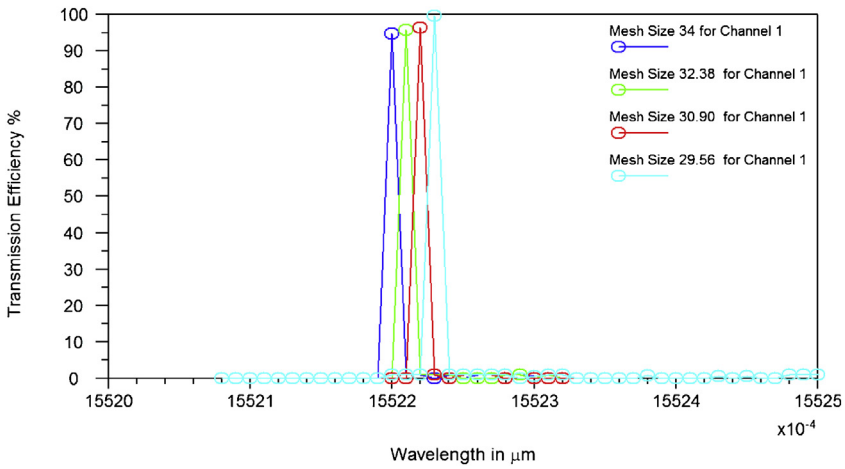

Fig. 5. Transmission spectrum of the proposed device for channel 1 for different mesh size.

the variation in each resonant wavelength shifts around more than 0.4 nm in the resonant wavelength and fabrication in optimizing both inner hole air holes and AHF make the system difficult. It is observed that increasing the radius of AHF by ±1.2 nm, a narrow wavelength was dropped with spectral line width of 0.2 nm and 0.4 nm in wavelength of the cavity.

To enhance the higher coupling efficiency and low cross talk between the channels. The width of drop waveguide for 25 GHz and 50 GHz channel 1 and channel 2 is widen to

$$DW1 = 2a \tag{11}$$

$$DW2 = 2a \tag{12}$$

a = lattice constant between two air holes.

The reverse engineering concept is used with many iterations after the detailed study of TE PBG 1 to optimize the radius of air holes, lattice constant, 6-AHF, and 7-AHF is used for optimizing the air hole's radius with the desired wavelength.

The integrated DWDM demultiplexer has 4 HRCs where each HRC is designed to drop two distinct wavelengths. Four HRCs are positioned between drop waveguide and bus waveguide. The input bus waveguide is designed with elimination of 27 air holes in the SOI lattice. Likewise, output drop waveguide is formed by eliminating 7 air holes in each channel. The hexagonal resonator is designed by eliminating 12 air holes. Two rows or single row of air holes act as coupling waveguide which is used to increase the coupling efficiency. The TE light enter in to coupling waveguide, it guide the light to AHF cavity through resonator. The proposed design uses the two row of air hole for the better coupling efficiency to resonator. The reflector (6 air holes) designed with the right end of the bus waveguide which enhances the coupling efficiency by 20%. The reflector produced the standing wave which is in a constructive interference with incident and reflected guided modes [44]. The reflector helps to enhance the signal strength from bus waveguide to resonator. At the resonant frequency, the back reflection of reflector inside the bus waveguide is utilized for coupling out through 6-AHF and 7-AHF point defect cavity. The defect cavity allows for the particular exit way to the channel to reduce the back reflection by 25%. The rest of the back reflection wave helps to improve the transmission efficiency.

5. Results and discussion

The propagation of light waves inside the SOI substrate for the designed demultiplexer is studied with Finite Difference Time Domain (FDTD) algorithm. The FDTD algorithm Perfect Matched Layer Absorbing Boundary Condition (PML ABC) is used to achieve higher rate of absorption in dissimilarity with the reflection of electromagnetic waves outside the simulating boundary region [45]. The PML ABC simulates under the condition of PML width and reflection as of 500 nm and 10^{-8}, which is the optimized value for good performance. The power monitor is placed at the end of each drop waveguide to measure the normalized transmission band. The transmission band is calculated with the equation:

$$T(f) = \frac{1/2 \int real\left(p(f)^{monitor}\right).dS}{SourcePower}. \tag{13}$$

Where $p(f)$ is the pointing vector, $T(f)$ denotes normalized transmission of frequency and ds denotes the surface normal to optimize the time step to work in both 25 GHz and 50 GHz DWDM environment. The FDTD algorithm uses the grid size as Δ = a/20 = 34 nm for the stable condition with the time step of Δt = $\Delta/\sqrt{2}c = 8.01387 \times 10^{-17}$ s. In the proposed design use, the time step for estimated FDTD (Δt) is of 8.01387×10^{-17}, The grid lattice updates the electric and magnetic field distribution in the finite time steps of Δt which have high accuracy during the propagation of a slow light wave inside the PCs [46]. The demultiplexer geometrical parameters are effective refractive index, lattice constant, and non defect air hole radius are of 2.83, 680 nm and 92 nm proportional to performance parameters like quality factor, transmission efficiency, and spectral line width, To obtain accurate transmission spectrum in the FDTD algorithm, it is necessary to choose the longer time step (10,000) for sharp peaks and lesser time leads to oscillations in the design. In the proposed design each wavelength is simulated for 250 min with the time step of grid size /8 to get the signal with high Q-factor in designing demultiplexer, which is given by

$$\Delta t \leq \frac{1}{c\sqrt{\frac{1}{\Delta X^2} + \frac{1}{\Delta Y^2}}} \tag{14}$$

The accuracy of FDTD technique is determined based on time step and mesh size. The sizes of the mesh size elements are very important for accurate geometry structure modeling. The smaller size of the mesh elements provides the more accurate model relevant to real time system. The proposed design is simulated for channel 1 with different mesh size such as, a/25, a/ 26, a/27 in order to understand the impact of geometry accuracy and stability of the proposed design.

The relation between resonant wavelength and mesh size is observed in the Figs. 5 and 6. From the Figs. 5 and 6, it is observed while increasing the 0.5 nm mesh size (a/20+ x, x = 0.5 nm), around

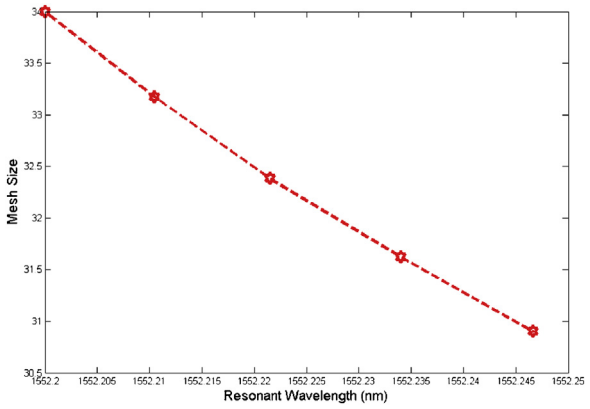

Fig. 6. Resonant wavelength vs. mesh size for the channel 1 (λ1 = 1552.2 nm).

0.01 nm resonant wavelength (1552.21 nm) shift is noticed. The smaller the mesh size gives the better accuracy with high simulation time. In this work, the mesh size chosen to be of a/20 is accounted to obtain stable output from different observations to get improved resolution. In addition, it is also noticed that there is a trivial variation in resonant wavelength and coupling efficiency, however it covers ITU standard DWDM demultiplexer. From the aforementioned results, it is observed that the proposed demultiplexer is meeting the requirement of the DWDM applications; hence, the proposed device could be implemented for the real time applications

The resonant frequencies show the slight change but even device continues to be an ITU standard DWDM demultiplexer with the same number with little deviation in coupling frequencies (0.01 nm). From the aforementioned results, it is observed that the proposed demultiplexer is meeting the requirement of the DWDM applications, hence, the proposed device could be implemented for the real time applications.

The refractive index of air/silicon on top layer is of 1/3.48 at 1550 nm and the refractive index of SiO_2 is of 1.45. The effective refractive index for the design is of 2.83. The 3D FDTD simulation is used for accurate modelling of the PC structure, but it requires more calculation time and high memory computers. So instead of 3D calculations it prefers to approximate with 2D for the effective index calculation of PC.

The structural parameters of the proposed demultiplexer (lattice constant, radius of the rod and refractive index of the material) are optimized in such a way that to get better performance. The proposed waveguide has 100% transmission efficiency in the range of 1387 nm < a/λ < 1942 nm. The degree of freedom for choosing holes radii ranging from 70 nm to 101 nm shows a better performance compared to below 70 nm air hole radii size. The design has constraint of choosing dielectric material, PC principle support only from the range of effective refractive index from 2 to 4. The effective refractive index less than 2 and greater than 4 will not follow the principle of PC dielectrical material. The proposed design must allow the proposed PBG design based on the geometrical parameters (radius of air hole, lattice constant, design, and effective refractive index).

In the four-channel integrated demultiplexer two channels are optimized to drop 25 GHz spectral line width spectrum whose resonant wavelengths are of 1552.2 nm and 1552.4 nm. The remaining two channels are designed to drop 50 GHz spectral line width spectrum whose resonant wavelengths are of 1554 nm and 1554.4 nm. The transmission spectrum of the integrated DWDM demultiplexer in uniform spectral linewidth is shown in Fig. 5.

The 25 GHz spectral line width spectrum is filtered from the hexagonal resonator by the 7-AHF. The radius of 7-AHF for channel C1 = 81.8 nm and C2 = 83 nm. After many iterations of the simulation, it is optimized and observed that for every ±1.2 nm increase in radius of air holes a shift is noticed in resonant wavelength with a spectral line width of 0.2 nm (25 GHz) and a channel spacing of 0.2 nm. Similarly, the 50 GHz spectral line width spectrum filter uses 6-AHF. The radius of 6-AHF for channel C1 = 89.2 nm and C2 = 90.4 nm. It is observed that for every ±1.2 nm increase in radius of air holes, a shift is noticed in the resonant wavelength with a spectral line width of 0.4 nm (50 GHz) and a channel spacing of 0.4 nm. The performance of integrated demultiplexer is listed in Table 1.

From the Table 1, it is given that maximum transmission efficiency, Q-factor and spectral line width are almost 100%, 7000 and 0.2 nm and 0.4 nm, respectively. Flexible spectral linewidth is obtained in the proposed design with the idea of increasing and reducing the number of air holes between hexagonal resonator and drop bus waveguide. One of the important parameters in designing a demultiplexer is extending the number of ports to support more number of users.

To maximize the number of integrated users we have extended the four-channel to eight-channel demultiplexer. In the extended eight-channel demultiplexer, the period lattice 38 × 38 is increased in X and Z direction. The design procedure is explained in detail in Section 2.

In the eight-channel integrated demultiplexer, four channels are optimized to drop 25 GHz spectral line width spectrum, whose resonant wavelengths are of 1551.4 nm, 1551.6 nm, 1551.8 nm, and 1552.0 nm with uniform spectral line width of 0.4 nm. Rest of four channels is designed to drop 50 GHz spectral line width spectrum whose resonant wavelengths are of 1556.3 nm, 1556.7 nm, 1557.1 nm, and 1557.5 nm. The transmission spectrum of eight-channel integrated DWDM demultiplexer in uniform spectral line width is shown in Fig. 6.

The 25 GHz spectral line width spectrum is filtered from the hexagonal resonator by the 7-AHF. The radii of 7-AHF for channel C1 = 77 nm, C2 = 78.4 nm, C3 = 79.4 nm, and C4 = 80.6 nm. After many iterations of the simulation, it is optimized and observed that for every ±1.2 nm increase in the radius of air holes a shift is noticed in the resonant wavelength with a spectral line width of 0.2 nm (25 GHz) and channel spacing of 0.3 nm. Similarly, the 50 GHz spectral line width spectrum is filtered from the hexagonal resonator by 6-AHF. The radii of 6-AHF for channel C1 = 95.6 nm, C2 = 96.8 nm, C3 = 98 nm, and C4 = 99.2 nm. It is observed that for every ±1.2 nm increase in radius of air holes, a shift is noticed in the resonant wavelength with the spectral line width of 0.4 nm (50 GHz) and channel spacing of 0.5 nm. The performance of integrated demultiplexer is listed in Table 2.

The multiplexed input Gaussian source travels through the bus waveguide. The device drops the resonant wavelength at the particular time only in one port as ON resonance remaining seven ports with zero light filed intensity as OFF resonance. Similarly, the corresponding resonant wavelength is dropped at its respective output port. At ON, resonance of the input signal is coupled from the bus waveguide to one of the resonators and its respective AHF to the drop waveguide. At OFF resonance, signal will not be coupled to the resonator. Figure 7(a) shows that first HRC channel 1 can drop the 25 GHz spectrum at the channel 1 λ_1= 1551.4 nm. A similar result can be seen in Fig. 7 (b) in which second HRC channel 2 can drop the 50 GHz spectrum at the channel 4 λ_4 = 1557.5 nm.

One of the significant factors in designing a demultiplexer is crosstalk (Cij). The crosstalk is evaluated between the adjacent channels. High Q-factor, transmission efficiency is obtained with low crosstalk. While designing an integrated demultiplexer, it is important to reduce the sidebands with the neighboring channels.

Figure 8 shows the output spectral response of transmission in dB, it is more convenient to identify the crosstalk. We find that the

Table 2
Resonant wavelength, cavity size, radius of defect air hole, spectral linewidth, Q-factor, and efficiency of the proposed eight-channel integrated demultiplexer.

Channel Spacing	Defect Radius (nm)	Cavity Size	DWDM CHANNELS		Spectral Line width ($\Delta\lambda$) in (nm)	Q-Factor	(%)
			6-AHF (50 GHz)	7 AHF (25 GHz)			
0.2 nm	77	588 nm	NA	λ_1 1551.4 nm	0.2	7756.5	90
	78.4	588 nm	NA	λ_2 1551.6 nm	0.2	7758	95
0.2 nm	79.4	588 nm	NA	λ_3 1551.8	0.2	7390	100
	80.6	588 nm	NA	λ_4 1552.0	0.2	7760	96
0.4 nm	95.6	680 nm	λ_1 1556.3	NA	0.4	3891	99
	96.8	680 nm	λ_2 1556.7	NA	0.4	3892	98
0.4 nm	98	680 nm	λ_3 1557.1	NA	0.4	3894	100
	99.2	680 nm	λ_4 1557.5 nm	NA	0.4	3896	98

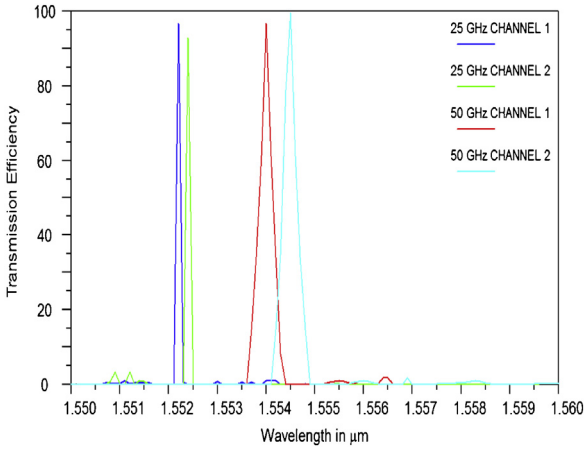

Fig. 7. Transmission spectrum for integrated four port demultiplexer (25 GHz Ch1 to Ch2 & 50 GHz Ch1 to Ch2) in Linear scale.

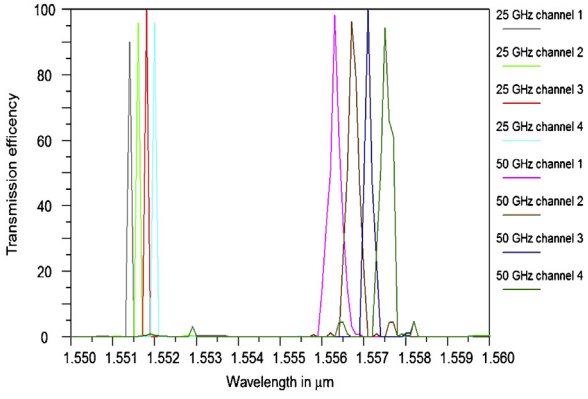

Fig. 8. Transmission spectrum for integrated eight-port demultiplexer (25 GHz Ch1 to Ch4 & 50 GHz Ch1 to Ch4) in linear scale.

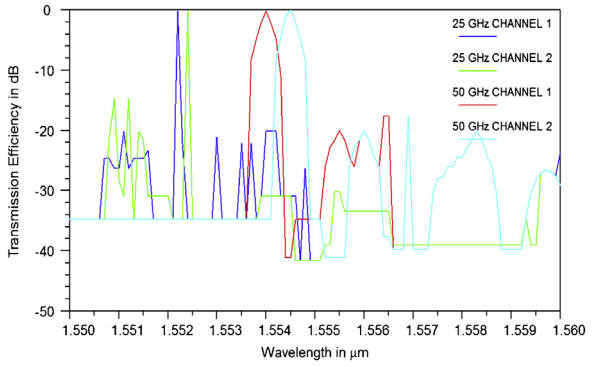

Fig. 10. Output spectral response of four-port demultiplexer (25 GHz Ch1 to Ch2 and 50 GHz Ch1 to Ch2) in dB.

Table 3
Crosstalk values (Cij) of proposed four-channel integrated demultiplexer (dB).

DWDM Channels (C_{ij})	λ_1 25 GHz	λ_2 25 GHz	λ_3 50 GHz	λ_4 50 GHz
λ_1 25 GHz	–	−31.56	−34.4	−34.2
λ_2 25 GHz	−34.77	–	−34.393	−34.39
λ_3 50 GHz	−34.85	−34.85	–	−24.72
λ_4 50 GHz	−34.6	−34.6	−23.79	–

transmission efficiency is good and the impact between the adjacent channels is not much serious. This is achieved in the proposed design with the optimal relation of lattice constant with the radius of air hole, optimized radius values for 6-AHF and 7-AHF, 5 rows of air holes between each channel, aforementioned factors provide the improvement by waveguides cut off frequency modulation which gives high Q-values (Figs. 9–11).

The crosstalk of the proposed eight channel demultiplexer is given in details in Tables 3 and 4. It is noticed that minimum crosstalk is observed, which is sufficient for the integrated DWDM demultiplexer in single slab.

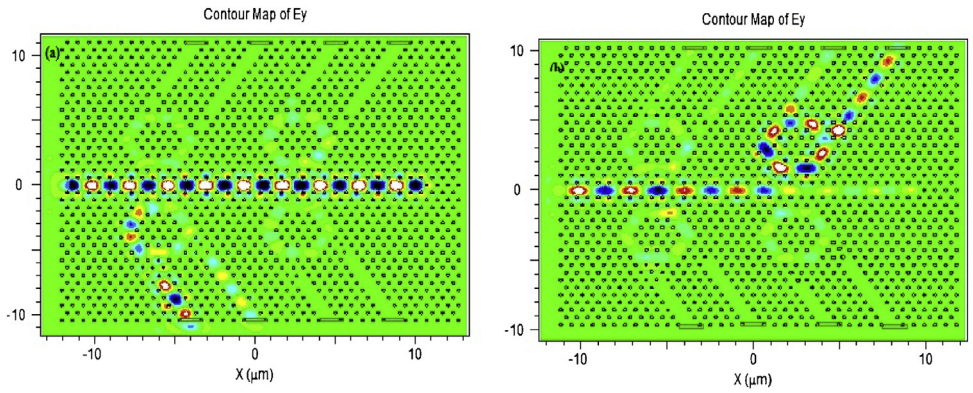

Fig. 9. Field distribution at channel 1 λ_1 = 1551.4 and channel 4 λ_4 = 1557.5 nm.

Table 4
Crosstalk values (Cij) of proposed integrated eight-channel demultiplexer (dB).

Channels (C_{ij})	λ_1 25 GHz	λ_2 25 GHz	λ_3 25 GHz	λ_4 25 GHz	λ_1 50 GHz	λ_2 50 GHz	λ_3 50 GHz	λ_4 50 GHz
λ_1 25 GHz	–	−31	−34.7	−34.6	−33.5	−34	−33	−33
λ_2 25 GHz	−30.9	–	−28.5	−27	−39	−39	−39	−39
λ_3 25 GHz	−34.4	−27	–	−34.27	−33	−33	−33	−33
λ_4 25 GHz	−34.68	−34.68	−34.68	–	−33.43	−38	−38	−38
λ_1 50 GHz	−34.68	−34.68	−34.68		−21	−33	−33	−33
λ_2 50 GHz	−34.6	−34.6	−34.6	−34.6	−33		−33.6	−39
λ_3 50 GHz	−34	−34	−34	−34	−33	−26.5	–	−23.7
λ_4 50 GHz	−34	−28	−22	−20	−33.6	−30.2	−21.5	–

The challenging parameter in designing of demultiplexer is crosstalk. The impact of crosstalk is serious in the optical communication in which a signal transmitted on one channel creates an undesired effect in another circuit or channel [47]. The demultiplexer gives the low crosstalk based on the structure of the resonator and the array of rod. Furthermore, the low crosstalk increases the Q-factor and the transmission efficiency. The crosstalk between the channels is calculated with:

$$\text{Crosstalk}\,(\text{dB}) = 10\log\frac{P_{out}}{P_{in}} \tag{15}$$

In Eq. (15), P_{out} represents the output power, P_{in} represents the input transmitted power of the system. Table 4 shows the crosstalk value for the proposed demultiplexer in dB. Crosstalk between channels is measured at the center of adjacent frequency from the desired resonant frequency.

The performance parameters such as transmission efficiency, spectral line width, Q-factor, footprint, channel spacing, ITU standard of previous works, and the results of the proposed integrated design are given in Table 5. Spectral line width, channel spacing, minimum crosstalk, Q-factor, footprint of the proposed demultiplexer are of 0.2 nm and 0.4 nm, 0.4 nm, −25 dB, 7000 and 481 μm^2, respectively. It is observed that the proposed integrated demultiplexer performs better than the existing demultiplexers. The aspects of hexagonal resonant cavity with two drop channels and HRCs being placed on both sides of the bus waveguide drastically reduce the size of the demultiplexer. To the best of our knowledge, it is the first attempt in designing an integrated

Table 5
Number of output ports, transmission efficiency, Q-factor, crosstalk, footprint, and channel spacing of the proposed demultiplexer is compared with existing triangular lattice and square lattice based demultiplexer.

Authors, Year, Reference no.	PC Lattice	No of Output Ports	T.E (%)	Crosstalk		Q-Factor	Footprint $(\mu m)^2$	Spectral linewidth (nm)	Integrated DWDM
			Min	Min	Max	Max			
2 CHANNEL									
M.Y. Tekeste et al. /2006/ [10]	T	2	100	NA	−14.2	65	NA	20 N.U.S.L	Single Model
S. Rawal et al. /2009/ [11]	T	2	89	NA	−7.5	NA	NA	24 N.U.C.L N_ITU	Single Model
4 CHANNEL									
A. Rostami et al./2009/ [22]	T	4	86.5	−21	−14.2	3912	536	1 U.S.L* N_ITU	Single Model
W. Liu et al./2012/ [23]	T	4	99	NA	−15	60	882	20 U.S.L ITU G 692	Single Model
H. Alipour-Banaei et al./2013/ [24]	T	4	63	−23.7	−11.2	1954	495	2.7 N.S.P.L N_ITU	Single Model
8 CHANNEL									
R. Talebzadeh et al./2017/ [32]	S	8	93	−46	−11	4320	2030	1 nm N.U.S.L N_ITU	Single Model
R.Talebzadeh et al./2017/ [33]	S	8	61	−36.5	−5	4860	790	1 nm N.U.S.L N_ITU	Single Model
F. Mehdizadeh et al./2015/ [34]	S	8	94	−40	−11.2	3842	495	0.4 N.U.S.L N_ITU	Single Model
12 CHANNEL									
V.R. Balaji et al./2016/ [36]	S	12	95	−42	−30	7890	784	0.2 U.S.L ITU	Single Model
Integrated Demultiplexer									
H. Tain et al./2013/ [37]	S	8	40	−26	−18	1000/200	882	0.8/20 N.U.S.L N_ITU	Integrated Model
Proposed Work	**T**	**8**	**99**	**-34**	**-21**	**7758/3896**	**481**	**0.2/0.4**	**Integrated Model**

T.E = Transmission efficiency.
U.S.L = Uniform Spectral Linewidth spacing for dropped wavelengths.
N.U.S.L = Non Uniform Spectral Linewidth spacing for dropped wavelengths.
N.U.C.L = Non Uniform Channel Spacing.
T→ Triangular lattice, S→ Square Lattice ITU→ International Telecommunication Union, N_ITU-Non International Telecommunication Union.

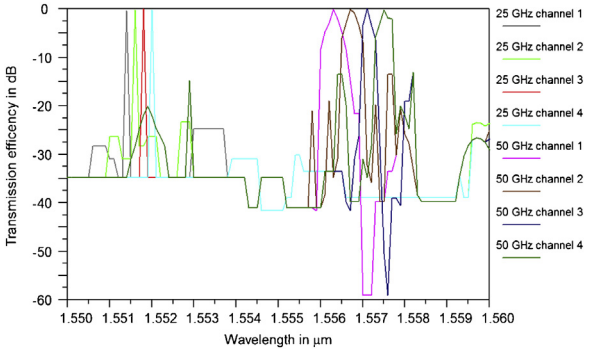

Fig. 11. Output spectral response of eight-port demultiplexer (25 GHz Ch1 to Ch4 & 50 GHz Ch1 to Ch4) in dB.

demultiplexer, which comprises features like ITU-T G.694.1 DWDM standard (25 GHz/50 GHz), uniform spectral line width, good transmission efficiency, high Q-factor. These attributes are essential for practical applications and can be implemented for future dual integrated systems.

6. Conclusions

In this paper, the hexagonal resonant cavity based 2DPCs with four-channel and eight-channel integrated demultiplexer is designed to work with ITU-T G.649.1 DWDM systems. The demultiplexer is designed to drop both 0.2 nm and 0.4 nm spectrum line widths in a single slab. By increasing the number of air holes between the resonant cavity and the drop waveguide, demultiplexer is able to drop narrow wavelength with high Q-factor. The desired wavelength is dropped through selecting the unique radius of the air hole in the 6-AHF/7-AHF filter. The proposed structure depicts appealing aspects for optical communication like dual frequency demultiplexer, 98% of transmission efficiency, −38 dB of the crosstalk 0.2 nm/0.4 nm uniform spectral line width, uniform channel spacing. The above-mentioned characteristics distinguishes the proposed integrated model from the existing models. The footprint of the designed demultiplexer is of 481 μm^2 which could be integrated for the integrated optics.

Conflict of interests

There is no conflict of interests regarding the publication of this paper.

References

[1] R. Saunders, Coherent DWDM technology for high speed optical communications, Opt. Fiber Technol. 17 (2011) 445–451.
[2] K.V. Shanthi, S. Robinson, Two-dimensional photonic crystal based sensor for pressure sensing, Photonic Sens. 4 (2014) 248–253.
[3] M. Bayindir, B. Temelkuran, E. Ozbay, Photonic-crystal-based beam splitters, Appl. Phys. Lett. 77 (2000) 3902–3904.
[4] S. Mandal, X. Serey, D. Erickson, Nanomanipulation using silicon photonic crystal resonators, Nano Lett. 10 (2009) 99–104.
[5] A. Locatelli, D. Modotto, D. Paloschi, C. De Angelis, All optical switching in ultrashort photonic crystal couplers, Opt. Commun. 237 (2004) 97–102.
[6] H. Kosaka, T. Kawashima, A. Tomita, T. Sato, S. Kawakami, Photonic-crystal spot-size converter, Appl. Phys. Lett. 76 (2000) 268–270.
[7] S. Fan, P.R. Villeneuve, J.D. Joannopoulos, H.A. Haus, Channel drop filters in photonic crystals, Opt. Express 3 (1998) 4–11.
[8] Y. Zhai, H. Tian, Y. Ji, Slow light property improvement and optical buffer capability in ring-shape-hole photonic crystal waveguide, J. Lightwave Technol. 29 (2011) 3083–3090.
[9] S.G. Johnson, P.R. Villeneuve, S. Fan, J.D. Joannopoulos, Linear waveguides in photonic-crystal slabs, Phys. Rev. B 62 (2000) 8212.
[10] M.Y. Tekeste, J.M. Yarrison-Rice, High efficiency photonic crystal based wavelength demultiplexer, Opt. Express 14 (2006) 7931–7942.
[11] S. Rawal, R.K. Sinha, Design and analysis and optimization of silicon-on-insulator photonic crystal dual band wavelength demultiplexer, Opt. Commun. 282 (2009) 3889–3894.
[12] H. Ghorbanpour, S. Makouei, 2-Channel all optical demultiplexer based on photonic crystal ring resonator, Front. Optoelectron. 6 (2013) 224–227.
[13] A. Pashaei, A. Andalib, H.A. Banaei, Decrease of crosstalk phenomenon optic two channel demultiplexer using resonant line defect cavity in 2D photonic crystal, Majlesi J. Telecommun. Devices 3 (2014) 35–40.
[14] A. Benmerkhi, M. Bouchemat, T. Bouchemat, Design of photonic crystal demultiplexer for optical communication application, Nanosci. Nanotechnol. 6 (2016) 29–34.
[15] H. Alipour-Banaei, S. Serajmohammadi, F. Mehdizadeh, Effect of scattering rods in the frequency response of photonic crystal demultiplexers, J. Optoelectron. Adv. Mater. 17 (2015) 259–263.
[16] H. Alipour-Banaei, S. Serajmohammadi, F. Mehdizadeh, Optical wavelength demultiplexer based on photonic crystal ring resonators, Photon. Netw. Commun. 29 (2015) 146–150.
[17] M. Koshiba, Wavelength division multiplexing and demultiplexing with photonic crystal waveguide couplers, J. Lightwave Technol. 19 (2001) 1970–1975.
[18] T. Niemi, L.H. Frandsen, K.K. Hede, A. Harpoth, P.I. Borel, M. Kristensen, Wavelength-division demultiplexing using photonic crystal waveguides, IEEE Photon. Technol. Lett. 18 (2006) 226–228.
[19] M. Djavid, F. Monifi, A. Ghaffari, M.S. Abrishamian, Heterostructure wavelength division demultiplexers using photonic crystal ring resonators, Opt. Commun. 281 (2008) 4028–4032.
[20] M.R. Rakhshani, M.A. Mansouri-Birjandi, Heterostructure four channel wavelength demultiplexer using square photonic crystals ring resonators, J. Electromagn. Waves Appl. 26 (2012) 1700–1707.
[21] A. Zahedi, F. Parandin, M.M. Karkhanehchi, H.H. Shams, S. Rajamand, Design and simulation of optical 4-channel demultiplexer using photonic crystals, J. Opt. Commun. (2017) 0039, http://dx.doi.org/10.1515/joc-2017-0039.
[22] A. Rostami, F. Nazari, H.A. Banaei, A. Bahrami, A novel proposal for DWDM demultiplexer design using modified-T photonic crystal structure, Photon. Nano Fundam. Appl. 8 (2010) 14–22.
[23] W. Liu, D. Yang, H. Tian, Y. Ji, Optimization transmission of photonic crystal coupled cavity and design of demultiplexer for wavelength division multiplexing application, Opt. Eng. 51 (2012), 084002-1.
[24] H. Alipour-Banaei, F. Mehdizadeh, S. Serajmohammadi, A novel 4-channel demultiplexer based on photonic crystal ring resonators, Optik 124 (2013) 5964–5967.
[25] C.W. Kuo, C.F. Chang, M.H. Chen, S.Y. Chen, Y.D. Wu, A new approach of planar multi-channel wavelength division multiplexing system using asymmetric super-cell photonic crystal structures, Opt. Express 15 (2007) 198–206.
[26] M.R. Rakhshani, M.A. Mansouri-Birjandi, Z. Rashki, Design of six channel demultiplexer by heterostructure photonic crystal resonant cavity, Int. Res. J. Appl. Basic Sci. 4 (2013) 976–984.
[27] A. Sharkawy, S. Shi, D.W. Prather, Multichannel wavelength division multiplexing with photonic crystals, Appl. Opt. 40 (2001) 2247–2252.
[28] S. Bouamami, R. Naoum, New version of seven wavelengths demultiplexer based on the microcavities in a two-dimensional photonic crystal, Optik 125 (2014) 7072–7074.
[29] K. Venkatachalam, D.S. Kumar, S. Robinson, Performance analysis of 2D-photonic crystal based eight channel wavelength division demultiplexer, Optik 127 (2016) 8819–8826.
[30] K. Venkatachalam, D.S. Kumar, S. Robinson, Investigation on 2D photonic crystal-based eight channel wavelength-division demultiplexer, Photon. Netw. Commun. 34 (2017) 100–110.
[31] K. Venkatachalam, D.S. Kumar, S. Robinson, Design and analysis of dual ring resonator based 2D-photonic crystal WDDM, Proceedings of AIP Conference 1849 (2017), 020016-1-020016-3.
[32] R. Talebzadeh, M. Soroosh, Y.S. Kavian, F. Mehdizadeh, All-optical 6-and 8-channel demultiplexers based on photonic crystal multilayer ring resonators in Si/C rods, Photon. Netw. Commun. (2017) 1–10.
[33] R. Talebzadeh, M. Soroosh, Y.S. Kavian, F. Mehdizadeh, Eight-channel all-optical demultiplexer based on photonic crystal resonant cavities, Optik 140 (2017) 331–337.
[34] F. Mehdizadeh, M. Soroosh, A new proposal for eight-channel optical demultiplexer based on photonic crystal resonant cavities, Photon. Netw. Commun. 31 (2016) 65–70.
[35] F. Shuai, W. Yi-Quan, Light propagation properties of two-dimensional photonic crystal channel filters with elliptical micro-cavities, Chin. Phys. B 20 (10) (2011), 104207.
[36] V.R. Balaji, M. Murugan, S. Robinson, Optimization of DWDM demultiplexer using regression analysis, J. Nanomater. (2016), 9850457.
[37] H. Tian, G. Shen, W. Liu, Y. Ji, Integration of both dense wavelength-division multiplexing and coarse wavelength-division multiplexing demultiplexer on one photonic crystal chip, Opt. Eng. 52 (2013), 076110-076110.
[38] V.R. Balaji, M. Murugan, S. Robinson, R. Nakkeeran, Design and optimization of photonic crystal based eight channel dense wavelength division multiplexing demultiplexer using conjugate radiant neural network, Opt. Quant. Electron. 49 (2017) 198.
[39] Z.Y. Li, L.L. Lin, Photonic band structures solved by a plane-wave-based transfer-matrix method, Phys. Rev. E 67 (2003), 0466067.
[40] D.M. Sullivan, An unsplit step 3-D PML for use with the FDTD method, IEEE Microw. Wirel. Compon. Lett. 7 (1997) 184–186.

[41] D.M. Sullivan, A simplified PML for use with the FDTD method, IEEE Microw. Guided Wave Lett. 6 (1996) 97–99.
[42] P.R. Villeneuve, S. Fan, J.D. Joannopoulos, Microcavties in photonic crystals: mode symmetry, tunability, and coupling efficiency, Phys. Rev. B 54 (1996) 7837–7839.
[43] E.H. Khoo, A.Q. Liu, J.H. Wu, J. Li, D. Pinjala, Modified step theory for investigating mode coupling mechanism in photonic crystal waveguide taper, Opt. Express 14 (2006) 6035–6054.
[44] K. Sangin, I. Park, H. Lim, S.Ch. Kee, Highly efficient photonics crystal-based multichannel drop filters of three-port system with reflection feedback, Opt. Express 22 (2004) 5518–5525.
[45] A. Lavrinenko, P.I. Borel, L.H. Fradsen, M. Thorhauge, A. Harpoth, M. Kristensen, T. Niemi, H.M.H. Chong, Comprehensive FDTD modeling of photonic crystal waveguide components, Opt. Express 12 (2004) 234–248.
[46] S.T. Chu, S.K. Chaudhuri, A finite-difference time-domain method for the design and analysis of guided-wave optical structures, J. Light Wave Technol. 7 (1989) 2033–2038.
[47] Y. Shen, K. Lu, W. Gu, Coherent and incoherent crosstalk in WDM optical networks, J. Light Wave Technol. 17 (1999) 759–764.